JOURNAL OF BACTERIOLOGY, Oct. 1992, p. 6033–6045
0021-9193/92/196033-13$02.00/0

Vol. 174, No. 19

Characterization of the Complex *pdxH-tyrS* Operon of *Escherichia coli* K-12 and Pleiotropic Phenotypes Caused by *pdxH* Insertion Mutations

HON-MING LAM AND MALCOLM E. WINKLER*

Department of Microbiology and Molecular Genetics, University of Texas Medical School, Houston, Texas 77030

Received 4 May 1992/Accepted 31 July 1992

We report the first molecular genetic analysis of a pyridoxine 5′-phosphate oxidase, the PdxH gene product of *Escherichia coli* K-12. Chromosomal insertions in and around *pdxH* were generated with various transposons, and the resulting phenotypes were characterized. The DNA sequence of *pdxH* was determined, and the promoters of *pdxH* and the downstream gene *tyrS*, which encodes tyrosyl-tRNA synthetase, were mapped by RNase T_2 protection assays of chromosomal transcripts. These combined approaches led to the following conclusions: (i) *pdxH* is transcribed from a sigma 70-type promoter and shares its transcript with *tyrS*; (ii) *tyrS* is additionally transcribed from a relatively strong, nonconventional internal promoter that may contain an upstream activating sequence but whose expression is unaffected by a *fis* mutation; (iii) PdxH oxidase is basic, has a molecular mass of 25,545 Da, and shares striking homology (>40% identity) with the developmentally regulated FprA protein of *Myxococcus xanthus*; (iv) mild pyridoxal 5′-phosphate limitation of *pdxH* mutants inhibits cell division and leads to formation of unsegregated nucleoids; (v) *E. coli* PdxH oxidase is required aerobically and anaerobically, but second-site suppressors that replace *pdxH* function entirely can be isolated; and (vi) *pdxH* mutants excrete significant amounts of L-glutamate and a compound, probably α-ketoisovalerate, that triggers L-valine inhibition of *E. coli* K-12 strains. These findings extend earlier observations that pyridoxal 5′-phosphate biosynthetic and aminoacyl-tRNA synthetase genes are often members of complex, multifunctional operons. Our results also show that loss of *pdxH* function seriously disrupts cellular metabolism in unanticipated ways.

Pyridoxal 5′-phosphate (PLP) and pyridoxamine 5′-phosphate (PMP) are important coenzymes that participate in many metabolic reactions, especially those involving amino acids (5, 22, 58). PLP and PMP are synthesized from pyridoxine (PN; vitamin B_6), pyridoxal (PL), and pyridoxamine (PM) by phosphorylation and oxidation reactions catalyzed by PN kinase (PN/PL/PM kinase; pyridoxal kinase; EC 2.7.1.35) and PNP oxidase (PNP/PMP oxidase; pyridoxaminephosphate oxidase; EC 1.4.3.5), respectively (Fig. 1) (15, 55). Of the three precursors, PN is thought to be the direct biosynthetic intermediate of PLP and is synthesized by bacteria, fungi, and higher plants (55). The biosynthesis of PN seems to occur by a branched pathway in *Escherichia coli* K-12 (33, 34) and most likely utilizes 4-hydroxythreonine (15, 33) and D-1-deoxyxylulose (23) as key intermediates. The last steps of PLP biosynthesis that take PN to PLP and PMP and interconvert the six B_6 vitamers (Fig. 1) seem to be present in all organisms (55).

The enzymology of eukaryotic PNP oxidase has been thoroughly studied in pig and sheep brain and rabbit liver (10, 11, 29, 36). Eukaryotic PNP oxidase is composed of two identical subunits (11, 29), and one flavin mononucleotide (FMN) molecule is bound to each dimer (11). Molecular oxygen is thought to be the sole electron acceptor in the oxidase reaction (29, 40). The oxidase seems to act preferentially on phosphorylated substrates (60) and is subject to product inhibition by PLP (Fig. 1) (60) that is reduced by partial proteolysis (30). Fluorescence polarization and resonance energy transfer studies suggest that there are protein-protein interactions between eukaryotic PNP oxidase and PN kinase (32).

Compared to the eukaryotic enzyme, relatively little has been reported about the biochemistry or genetics of prokaryotic PNP oxidase, which is encoded by *pdxH* at 36 min in the *E. coli* genetic map (15). Preliminary enzymological characterization in crude extracts suggested that *E. coli* PNP oxidase may be a flavoprotein that utilizes molecular oxygen as a substrate for at least 80% of its activity (56). However, interpretation of kinetic data was extremely difficult because of phosphatases in crude extracts which destroyed the PLP product. Point and Mu*dI*-8 insertion mutations in *pdxH* were isolated in both *E. coli* K-12 (25, 33) and *E. coli* B (14) strains by exploiting the property that *pdxH* mutants deficient in PNP oxidase grow on medium supplemented with PL but not with PN (Fig. 1). Recently, we reported the cloning of *E. coli* K-12 *pdxH*$^+$ (33). Complementation analysis of all known *pdxH* mutants demonstrated that *pdxH* consists of a single complementation group.

Here we report a structural analysis of the *pdxH* gene and its chromosomal transcription. Our data show that *pdxH*, like other *pdx* genes involved in PN biosynthesis (2, 17, 33, 34, 44, 54), forms a complex operon with a downstream gene, in this case, *tyrS*, which encodes the essential enzyme tyrosyl-tRNA synthetase (48). Physiological characterization of *pdxH* mutants revealed several unusual phenotypes, including a block in nucleoid segregation and cell division and excretion of L-glutamate (L-Glu) and a compound that inhibits L-isoleucine (L-Ile) biosynthesis. The absence of growth of *pdxH* insertion mutants aerobically and anaerobically, except when supplemented with PL, suggested that the PdxH enzyme is required for PLP biosynthesis in wild-

* Corresponding author. Electronic mail address: mwinkler@utmmg.med.uth.tmc.edu

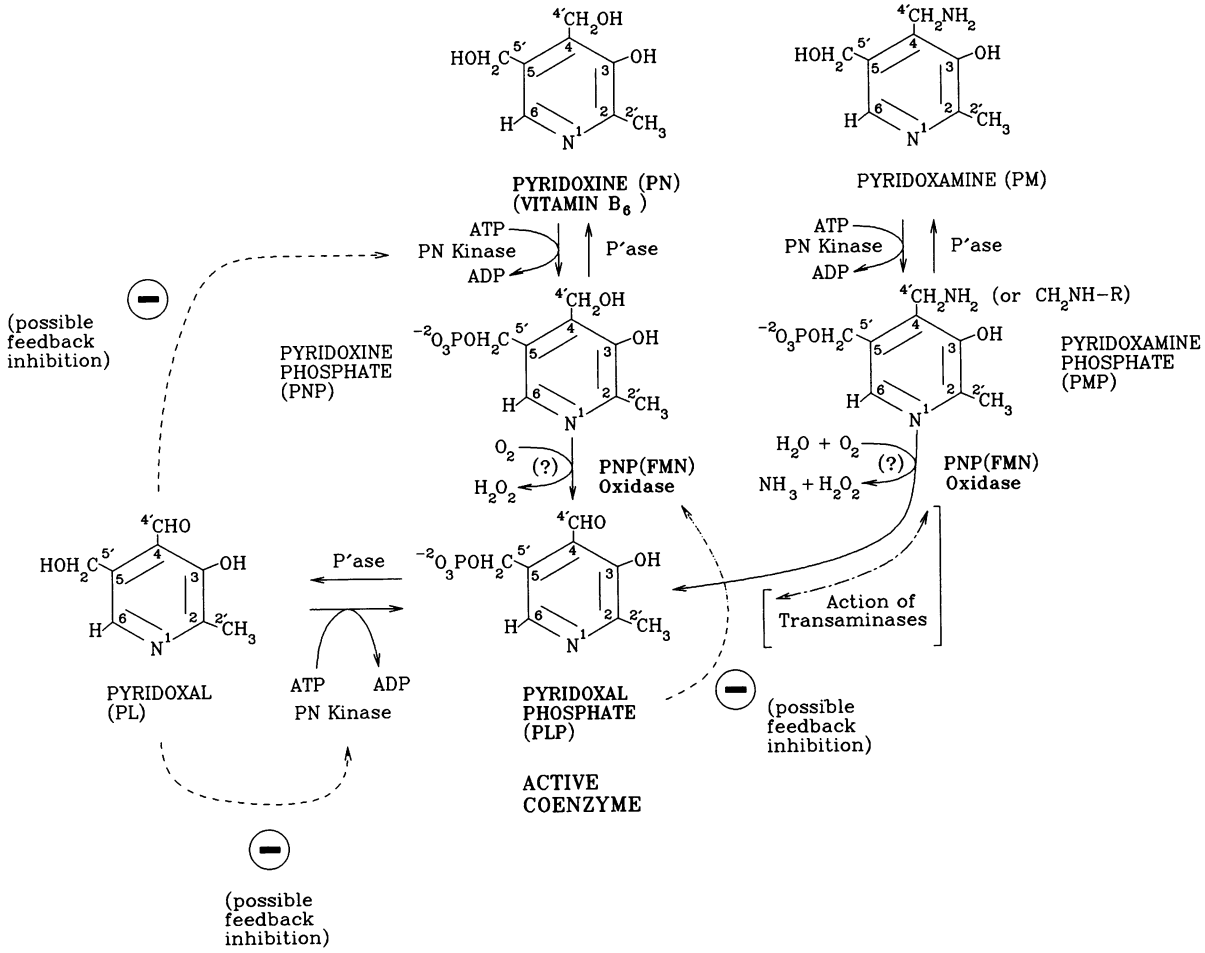

FIG. 1. Universal biosynthetic pathways leading from PN (vitamin B_6) to active PLP coenzyme and allowing interconversion of the six B_6 vitamers. The scheme is based on data reviewed in references 15 and 55. The minus signs indicate points of probable negative feedback inhibition of enzyme activities (36, 62). Alternative names for PN kinase (EC 2.7.1.35) and PNP oxidase (EC 1.4.3.5) include PN/PL/PM kinase, pyridoxal kinase, and PdxK kinase (in *E. coli*) and PNP/PMP oxidase, pyridoxaminephosphate oxidase, and PdxH oxidase (in *E. coli*), respectively.

type cells. However, isolation of suppressors that replace *pdxH* function suggests the presence of an alternative pathway or form of oxidase for PN oxidation in *E. coli*.

MATERIALS AND METHODS

Materials. The following enzymes and reagents were used in cloning, DNA sequencing, strain construction, and RNase T_2 transcript mapping experiments: restriction endonucleases, phosphorylated *Sph*I and *Bam*HI linkers, and M13 sequencing (−40) primer (New England Biolabs, Beverly, Mass., and Promega, Madison, Wis.); Riboprobe Gemini System II, restriction endonucleases, RQ1 DNase, and plasmid pGEM-3Z (Promega); RNase T_2 and bacterial alkaline phosphatase (Bethesda Research Laboratories, Gaithersburg, Md.); 17-mer oligonucleotide primers for DNA sequence determinations (Genosys, Inc., Woodlands, Tex.); T4 DNA polymerase (Boehringer Mannheim Biochemicals, Indianapolis, Ind.); pyrophosphatase and Sequenase (version 2.0) sequencing kits (United States Biochemical, Cleveland, Ohio); and Thermalbase sequencing kit (Stratagene, La Jolla, Calif.). Other chemicals used in these experiments included the following: radioactive compounds (Amersham Corp., Arlington Heights, Ill.); inorganic salts, organic solvents, BBL Gas-Pak supplies, and electrophoresis-grade agarose (Fisher Scientific, Fair Lawn, N.J.); acrylamide-bisacrylamide mixtures (29:1) (Curtin Matheson Scientific, Inc., Houston, Tex.); and ammonium persulfate and TEMED (*N,N,N',N'*-tetramethylethylenediamine) (Bio-Rad, Inc., Richmond, Calif.). Chemicals used for other experiments were DAPI (4',6-diamino-2-phenylindole); polylysine solution, antibiotics, and biochemicals (Sigma Chemical Co., St. Louis, Mo.); and glutamate dehydrogenase (Boehringer Mannheim Biochemicals). Ingredients for culture media included vitamin assay Casamino Acids, Bacto-Agar, yeast extract, and tryptone broth (Difco Laboratory, Detroit, Mich.).

Bacterial strains and plasmids. Bacterial strains, plasmids, and phages used in this study are listed in Table 1. P1 bacteriophage generalized transductions and 2-aminopurine mutagenesis of cells were carried out as described in reference 37. Recombinant plasmids were constructed by standard techniques (3, 46). Insertional mutagenesis of plasmids with mini-Mu*d*II elements was performed as previously described (9). Insertion positions in plasmids harboring mini-Mu*d*II elements were determined by restriction analy-

TABLE 1. Bacterial strains and plasmids

Strain or plasmid	Phenotype or genotype[a]	Source or reference
Strains		
DS941	*fis*::Km^r F$^-$ *ara-14 argE3 galK2 his-4 lacI^q lacZ*Δ*M15 leu-6 mtl-1 proA2 recF143 str-31 supE44 thi-1 thr-1 tsx-33 xyl-5*	J. Hinton collection
JC7623	*recB21 recC22 sbc-15 ara arg his leu pro thr*	A. J. Clark collection
NU816	W3110 Δ*lacU169 tna2 sup*^{0}	C. Yanofsky collection
NU887	SVS1100 *pdxH*::Mu*d*I-8-1	SVS1100 transposed with a Mu*d*I-8 element
NU901	SVS1100 *pdxA*::Mu*d*I-8	SVS1100 transposed with a Mu*d*I-8 element
NU908	SVS1100 *pdxH*::Mu*d*I-8-2	SVS1100 transposed with a Mu*d*I-8 element
NU1707	NU816 *pdxH*::Mu*d*I-8-1	NU816 × P1*kc*(NU887)
NU1708	NU816 *pdxH*::Mu*d*I-8-2	NU816 × P1*kc*(NU908)
NU1709	NU816 *pdxA*::Mu*d*I-8	NU816 × P1*kc*(NU901)
NU1730	NU1707(pNU216)	Transformant
NU1732	NU1708(pNU216)	Transformant
NU1735	NU1707(pNU217)	Transformant
NU1736	NU1708(pNU217)	Transformant
NU1737	JC7623 *zbe*::mini-Mu*d*II-3	JC7623 × linear pNU267
NU1738	JC7623 *zbe*::mini-Mu*d*II-2	JC7623 × linear pNU268
NU1739	JC7623 *zbe*::mini-Mu*d*II-1	JC7623 × linear pNU269
NU1740	JC7623 *zbe*::mini-Mu*d*II-4	JC7623 × linear pNU270
NU1814	NU816(pNU216)	Transformant
NU1815	NU816(pNU217)	Transformant
NU1833	NU816 *zbe*::mini-Mu*d*II-3	NU816 × P1*kc*(NU1737)
NU1835	NU816 *zbe*::mini-Mu*d*II-2	NU816 × P1*kc*(NU1738)
NU1837	NU816 *zbe*::mini-Mu*d*II-1	NU816 × P1*kc*(NU1739)
NU1839	NU816 *zbe*::mini-Mu*d*II-4	NU816 × P1*kc*(NU1740)
SVS1100	*bglR551* Δ(*lac-argF*)*U169*	V. Stewart collection
TT6547	*supD ara-14 eda-50* Δ*lacU169 metF*(Am) *mtl-1 rpsL136 thi-1 tonA31 tsx-78 xyl-5*	J. Roth (26)
TT9894	TR6547 Muc62ts Mu*d*I-8 dilysogen	J. Roth (26)
TX2268	NU816(pTX281)	Transformant
TX2277	NU1707(pTX281)	Transformant
TX2278	NU1708(pTX281)	Transformant
TX2351	NU816(pBR325)	Transformant
TX2361	JC7623 ORF1::Km^r(*Sph*I)>	JC7623 × linear pTX294
TX2362	JC7623 ORF1::<Km^r(*Sph*I)	JC7623 × linear pTX295
TX2363	NU816 ORF1::Km^r(*Sph*I)>	NU816 × P1*vir*(TX2361)
TX2364	NU816 ORF1::<Km^r(*Sph*I)	NU816 × P1*vir*(TX2362)
TX2451	NU816 *fis*::Km^r	NU816 × P1*vir*(DS941)
Plasmids		
pBR325	ColE1 replicon; Ap^r Tc^r Cm^r	Lab stock (8)
pGEM-3Z	Vector for riboprobe synthesis; Ap^r	Promega
pMB2190	Km^r in pBR327 derivative; Ap^r Tc^r	B. Nichols collection
pNU216	ORF1-*pdxH*$^+$ cloned in pBR325; Ap^r Cm^r	Lab stock (33)
pNU217	*pdxH*$^+$-*tyrS*$^+$ cloned in pBR325; Ap^r Cm^r	Lab stock (33)
pNU267	pNU217 (*zbe*::mini-Mu*d*II-1); *pdxH*$^+$; Ap^r Cm^r	This work
pNU268	pNU217 (*zbe*::mini-Mu*d*II-2); *pdxH*$^+$; Ap^r Cm^r	This work
pNU269	pNU217 (*zbe*::mini-Mu*d*II-3); *pdxH*$^+$; Ap^r Cm^r	This work
pNU270	pNU217 (*zbe*::mini-Mu*d*II-4); *pdxH*$^+$; Ap^r Cm^r	This work
pTX281	pBR325 containing a 1.8-kb *Sph*I-*Bam*HI fragment from pNU217; *pdxH*$^+$; Ap^r Cm^r	This work
pTX292	pBR325 lacking *Sph*I site	This work
pTX293	pTX292 containing a 5.4-kb *Bam*HI-*Bam*HI fragment from pNU216 *pdxH*$^+$; Ap^r Cm^r	This work
pTX294	pTX293 ORF1::Km^r(*Sph*I)> *pdxH*$^+$; Ap^r Cm^r	This work
pTX295	pTX293 ORF1::<Km^r(*Sph*I) *pdxH*$^+$; Ap^r Cm^r	This work
pTX303	0.57-kb *Ava*I-*Sac*II fragment from pTX281 cloned into the *Bam*HI site of pGEM-3Z; *pdxH* transcription same orientation as *lacZ*; Ap^r	This work
pTX306	0.76-kb *Sac*II-*Sph*I fragment from pTX281 cloned into the *Bam*HI site of pGEM-3Z; *pdxH* transcription same orientation as *lacZ*; Ap^r	This work

[a] < or > indicates that the direction of transcription of *kan* in the Km^r cassette is opposite to or the same as that of *pdxH*, respectively. Km^r(*Sph*I) signifies the presence of a kanamycin resistance cassette cloned into the *Sph*I site of ORF1 (Fig. 2). mini-Mu*d*II-1-4 mapped immediately downstream from *tyrS* (Fig. 2). The mini-Mu*d*II-2 element in NU1835 (Fig. 2) was in the opposite orientation as *tyrS* but formed an active *lacZ* gene fusion. Ap^r, ampicillin resistant; Cm^r, chloramphenicol resistant; Tc^r, tetracycline resistant.

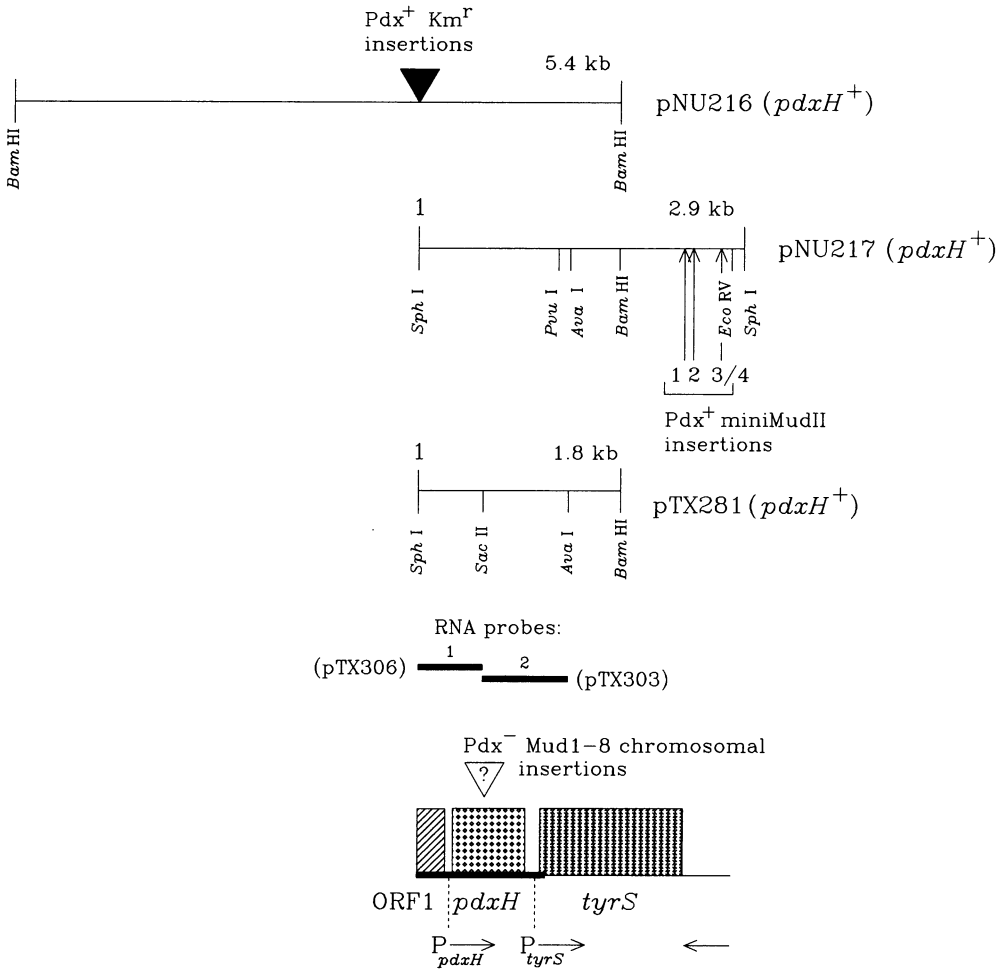

FIG. 2. *pdxH*$^+$ recombinant plasmids and locations of insertion mutations in and around *pdxH* in recombinant plasmids and the *E. coli* K-12 chromosome. The whole figure is drawn to scale. *pdxH*::Mu*d*I-8, ORF1::Km^r, and *zbe*::mini-Mu*d*II insertions were isolated or constructed and crossed into the bacterial chromosome as described in Materials and Methods. Exact positions of Mu*d*I-8 elements within *pdxH* are unknown. Restriction mapping showed that the *zbe*::mini-Mu*d*II elements were extremely close to the end of *tyrS*. *zbe*::mini-Mu*d*II-2 formed active *lacZ* gene fusions but was in the opposite orientation to *tyrS*. The positions of the two RNA probes used to map in vivo transcripts are indicated. The dark black line in the summary diagram at the bottom marks the new DNA sequence reported in Fig. 3. The positions and identities of the reading frames and promoters are based on data presented here and in reference 4 for the *tyrS* coding region. No transcription was detected in vivo from either DNA strand in the 280-bp region upstream from *pdxH* (ORF1; see text).

ses. Kanamycin resistance cassettes with *Sph*I linkers at their ends were cloned in both orientations into the *Sph*I site in pTX293 to disrupt the open reading frame upstream from *pdxH* (ORF1, Fig. 2). Insertions imparting antibiotic resistances were crossed from linearized plasmids into the chromosome of *recBC sbc* mutant JC7623 as detailed before (1, 63) *pdxH*::Mu*d*I-8 chromosomal mutants and plasmids pNU216 and pNU217 were isolated previously in this laboratory (33). Plasmid pTX281 (Fig. 2) was constructed by subcloning the 1.8-kb *Sph*I-*Bam*HI fragment from pNU217 into pBR325. Plasmids pTX303 and pTX306, which were used for RNase T_2 protection assays, were constructed by ligating *Bam*HI linkers onto the 0.57-kb *Ava*I-*Sac*II and 0.76-kb *Sac*II-*Sph*I fragments from pTX281, respectively, and cloning the resulting fragments into the *Bam*HI site of vector pGEM-3Z.

Culture conditions. LBC rich medium was Luria-Bertani broth supplemented with 30 μg of L-cysteine per ml. Minimal Vogel-Bonner (1XE) medium containing 0.01 mM $FeSO_4$ was prepared as described in reference 13. MMG was 1XE salts plus 0.4% (wt/vol) glucose. Where specified, MMG was supplemented with 0.5% (wt/vol) vitamin assay Casamino Acids. PL was added to media at a final concentration of 1 μM. Other growth conditions are described in the figure legends and table footnotes.

DNA sequence analysis. DNA sequences were determined by the Sequenase and Thermalbase variations of the Sanger dideoxynucleotide method from single-strand mp18 and mp19 M13 phage clones (47) as described previously (44, 49). Both strands were sequenced with each enzyme or by using at least two different reaction mixtures containing dGTP, dITP, or deaza-dGTP according to the manufacturer's instructions. Synthetic primers were used to sequence along the M13 phage clones and to close all gaps. DNA sequences were analyzed with the University of Wisconsin Genetics Computer Group and PCGene (Intelligenetics, Inc., Moun-

tain View, Calif.) computer programs, which included access to the GenBank, EMBL, and Ecoseq (45) data bases.

RNase T_2 transcript analysis. RNase T_2 mapping of in vivo transcripts was performed as described previously (49) with the following changes: (i) total cellular RNA was prepared by a boiling lysis method in which cells were lysed directly in culture medium without centrifugation (18); (ii) the last step of the RNA purification included treatment with RQ1 (RNase-free) DNase (49); (iii) RNase T_2 digestion was carried out at 37°C for at least 4 h, instead of at 30°C; and (iv) after digestion with RNase T_2, samples were extracted with phenol-chloroform-isoamyl alcohol (24:23:1 by vol) and precipitated with 2 volumes of ethanol. After electrophoresis, gels were dried, and radioactive bands were quantitated with a beta scope (Betagen Corp., Waltham, Mass.).

Light microscopy, amino acid analyses, and L-glutamate bioassays. Cell morphologies were examined following DAPI staining using combined phase-contrast and fluorescence light microscopy as described in reference 24. Amino acid analyses were performed by the Analytical Chemistry Center of this university by using ion-exchange high-performance liquid chromatography (HPLC) provided as part of an automated Pharmacia-LKB system. Bioassay of L-glutamate by glutamate dehydrogenase activity was performed as described in reference 6.

Nucleotide sequence accession number. The GenBank accession number for the sequence in this paper is M92351.

RESULTS

Localization of *pdxH* by subcloning and insertion mutagenesis. We reported previously the isolation of *pdxH*::Mu*d*I-8 insertion mutants and two overlapping clones, pNU216 and pNU217, that complemented *pdxH* insertion and point mutations (Fig. 2) (33). We isolated one smaller subclone of pNU217 that still complemented *pdxH* mutants (pTX281, Fig. 2). DNA sequence analysis presented below conclusively demonstrated that plasmid pTX281 contained only one intact open reading frame that must correspond to the *pdxH*$^+$ gene (Fig. 2 and 3). Besides *pdxH*$^+$, pTX281 contained part of an upstream open reading frame (ORF1) and the first half of downstream *tyrS*, whose DNA sequence was reported previously (Fig. 2 and 3) (4).

Insertion mutagenesis confirmed the placement of *pdxH*$^+$ between ORF1 and *tyrS*. We introduced kanamycin resistance (Km^r) cassettes in both orientations into the *Sph*I site of plasmid pNU216 to disrupt ORF1 (Fig. 2). Insertions close to the end of *tyrS* were generated by transposition of mini-Mu*d*II(Km^r) elements into pNU217 (Fig. 2). The kanamycin resistance cassettes and mini-Mu*d*II insertion mutations were crossed into the bacterial chromosome via homologous recombination from linearized plasmid DNA (1, 63). All *pdxH*::Mu*d*I-8, ORF1::Km^r, and mini-Mu*d*II insertions were transduced into strain NU816 (W3110 Δ*lac*). The resulting strains were checked and found to lack plasmids, which is consistent with recombination of insertion elements into the bacterial chromosome.

Chromosomal *pdxH*::Mu*d*I-8 mutations caused a requirement for exogenous PL that could not be satisfied by PN (33). By contrast, chromosomal insertions in ORF1 upstream from *pdxH* or downstream from the end of *tyrS* did not show observable growth defects in LBC medium or MMG. These observations confirmed that ORF1 is not required for *pdxH* function. Strong polar effects of ORF1 or *pdxH* insertions on *pdxH* or *tyrS* expression would result in a PL requirement or impaired growth, respectively. Such strong polar effects were not observed, which suggested that *pdxH* and *tyrS* probably are expressed independently, at least under the growth conditions tested. The latter conclusion was confirmed by the transcription analysis presented below. Finally, one of the chromosomal mini-Mu*d*II insertions located downstream near the end of *tyrS* (NU1835, *zbe*::mini-Mu*d*II-2, Table 1; Fig. 2) formed an active *lacZ* gene fusion, as judged by deep red colony color on MacConkey-lactose plates. This gene fusion was in the opposite orientation to *pdxH* and *tyrS* (Fig. 2), consistent with transcription in the opposite direction to *pdxH* and *tyrS*.

DNA sequence analysis of *pdxH*. DNA sequence analysis delineated the genetic organization of *pdxH* and adjacent loci (Fig. 3). The open reading frame between nucleotides (nt) 310 and 966 was identified as the *pdxH* gene product on the basis of the genetic criteria described above. The translation start was assigned on the basis of the strong homology described below between *E. coli pdxH* and *Myxococcus xanthus fprA*. AUG at nt 310 is the only possible translation start that can accommodate this homology. The *pdxH* translation start contains a relatively poor match (three of six) to the Shine-Dalgarno ribosome-binding sequence (Fig. 3). Predicted properties of *E. coli* PdxH protein and comparisons with the eukaryotic enzyme are in the Discussion.

FASTA and TFASTA searches of EMBL-GenBank revealed a remarkable homology between *E. coli* PdxH and *M. xanthus* FrpA (Fig. 4) (20). Degrees of identity and overall similarity are about 43 and 64%, respectively, over the entire length of both polypeptides (Fig. 4). The *fprA* gene seems to be developmentally regulated in *M. xanthus* (20); however, no function was discovered for the FprA protein other than its ability to bind FMN tightly but not covalently (50). FMN binding is a property expected for PNP oxidase from enzymological characterizations of the purified eukaryotic enzyme (11) and activities in crude extracts of *E. coli* (see the introduction) (56). Together, the homology with the *E. coli* PdxH protein and its high affinity for FMN strongly suggest that *fprA* encodes PNP oxidase in *M. xanthus*. Possible ramifications of the developmental control of *fprA* to PLP biosynthesis are considered in the Discussion.

The unknown open reading frame immediately upstream from *pdxH* (ORF1; Fig. 2 and 3) matched a partial open reading frame of unknown function from *Yersinia enterocolitica* (ORF4'; GenBank accession X60449). However, chromosomal insertions in ORF1 failed to show discernible phenotypes (Fig. 2), and no chromosomal transcription from the ORF1 region was detected from either DNA strand in cells growing exponentially in LBC medium (see below). Consequently, we do not presently know the function, if any, of the 250 bp preceding the *pdxH* promoter (marked in Fig. 3; see below). In contrast, the open reading frame immediately downstream from the end of *pdxH* was readily identified as the essential *tyrS* gene, which encodes tyrosyl-tRNA synthetase (Fig. 2 and 3) (4). We demonstrate a relationship between *pdxH* and *tyrS* transcription in the next section.

Transcript mapping of *pdxH* and *tyrS* promoters. The close proximity of *pdxH* and *tyrS* prompted us to examine whether *pdxH* and *tyrS* share a transcript and constitute a complex operon. RNA probes 1 and 2 (Fig. 2) were synthesized corresponding to the ORF1-*pdxH* and *pdxH-tyrS* junctions, respectively, from both DNA strands as described in Materials and Methods. Total cellular RNA was purified from strain NU816 growing exponentially in LBC medium at 37°C with shaking and hybridized to the four RNA probes. Figure 5 shows the segments of the probes protected from RNase T_2

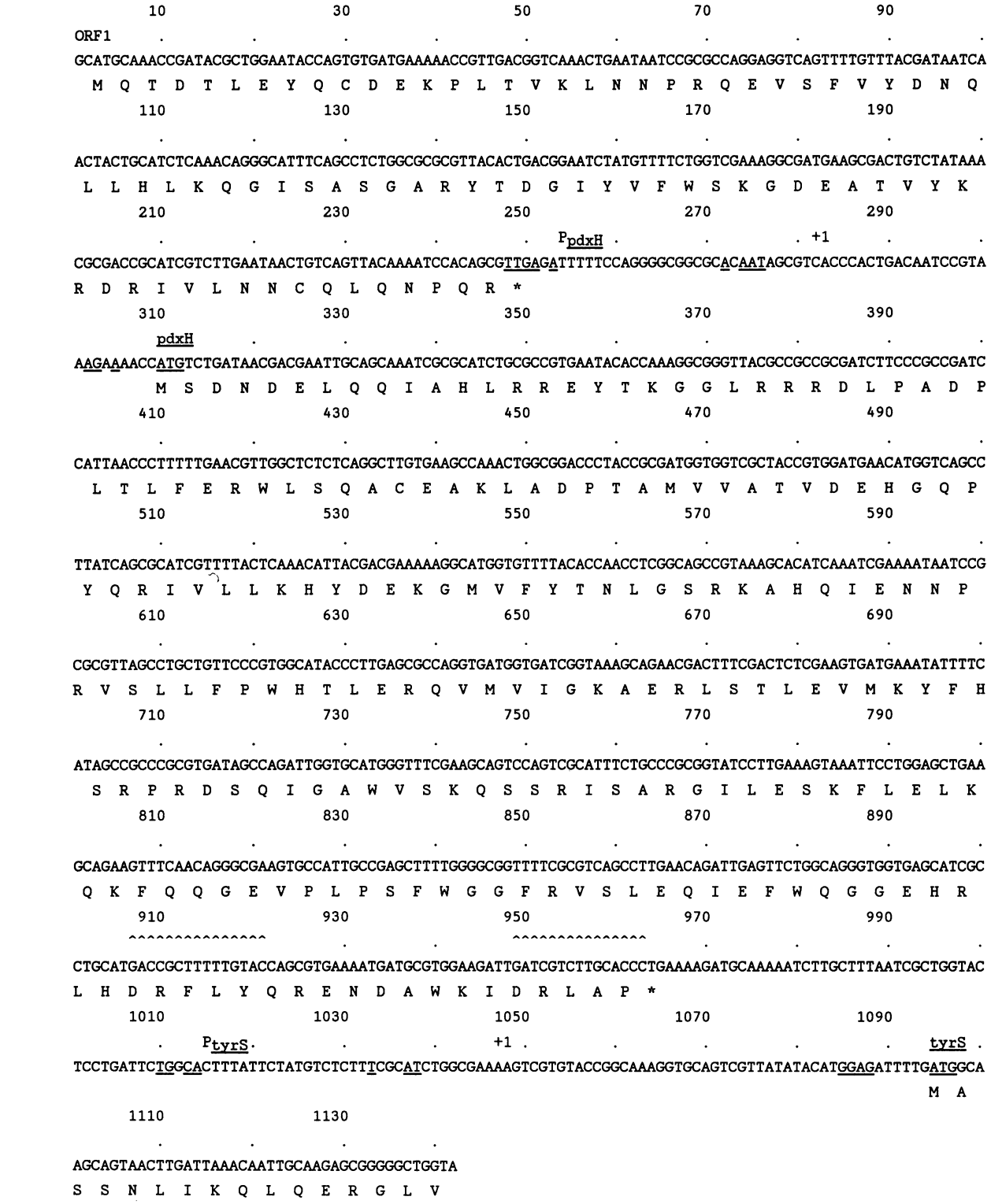

FIG. 3. DNA sequence of *pdxH* extending to the start of *tyrS*. The sequence is numbered from the *Sph*I site at the left end of the chromosomal insert in *pdxH*$^+$ recombinant clones pNU217 and pTX281 (Fig. 2). Probable transcription starts are indicated by +1. Likely σ-70 promoter consensus sequences, ribosome binding sites, and translation start codons are underlined. Two putative Fis protein binding sites are marked (^) in the A-T-rich region immediately upstream of P_{tyrS}. Transcript mapping experiments indicated that no transcription termination appears to occur between *pdxH* and *tyrS* (see Fig. 5 and 6). Other features of the DNA sequence are described in the text.

```
PdxH   7 LQQIAHLRREYTKGG.........LRRRDLPADPLTLFERWLSQACEAKLA 48
FprA   1 MRTLTCVPDESTAKVHTCRAPFMLHRVMIPPDPIQRFAELFERAKQAIAV 50
        49 DPTAMVVATVDEHGQPYQRIVLLKHYDEKGMVFYTNLGSRKAHQIENNPR 98
        51 DPNAMVVATVGDDGRPSARVVLLKDFDARGFVFYTNHESRKGREARAHPY 100
        99 VSLLFPWHTLERQVMVIGKAERLSTLEVMKYFHSRPRDSQIGAWVSKQSS 148
       101 AALCFYWQPLNEQVRVEGRVERVTDAEADAYFQSRARGSQVGAWASLQSQ 150
       149 RISARGILESKFLELKQKFQQGEVPLPSFWGGFRVSLEQIEFWQGGEHRL 198
       151 PLATREELEARVAEVEQKYAGQPVPRPPHWSGFRVVPDRIEFWHAQESRL 200
       199 HDRFLYQRENDAWKIDRLAP 218
       201 HDRHVYLREDGGWRTQMLYP 220
```

FIG. 4. Amino acid alignment between the *E. coli pdxH* gene product, PNP oxidase, and the *M. xanthus fprA* gene product, which is known to bind FMN. The *M. xanthus* sequence was reported by Hagen and Shimkets (20). The homology between PdxH and FprA was originally discovered in a FASTA search of EMBL-GenBank (initial alignment score = 475). The alignment in the figure was generated with the Bestfit program in the University of Wisconsin Genetics Computer Group software package. Degrees of identity and overall similarity are about 43 and 64%, respectively, over the entire length of both polypeptides. No obvious putative FMN and flavin adenine dinucleotide (41, 53), ferredoxin (64), or NAD (7) binding site motifs were detected in either enzyme. Likewise, a lysine-containing peptide similar to the one that reacts with bis-PLP in sheep brain (10) was not found in either protein. Relationships between amino acid pairs: |, identical; :, highly conserved; ., moderately conserved.

digestion. Undigested probes are in the odd-numbered lanes, and positions of additional RNA size standards are indicated. Hybridization of probe 1 corresponding to the *pdxH* noncoding strand showed one strong band with a size of 491 ± 5 nt (Fig. 5, lane 4). We interpret this band to represent transcription from a promoter immediately upstream from the translation start of *pdxH* (P_{pdxH}, Fig. 2 and 3). The most likely placement of P_{pdxH} indicates an almost perfect −35 σ-70 consensus region and a −10 region containing the most highly conserved A and T bases (Fig. 3). One somewhat unusual feature of P_{pdxH} is the runs of T and G residues between the −35 and −10 regions.

No transcription from the ORF1 region was detected with probe 1 *pdxH* noncoding or opposite strand (Fig. 5, lanes 4 and 2, respectively). In some experiments, gels were run so that even short protected fragments should have been detectable (data not shown). We interpret the faint band below the strong band in Fig. 5, lane 4, to represent a fragment corresponding to transcription from P_{pdxH} which was formed by slight overdigestion by RNase T_2. Its relatively large size (≈480 nt) makes it unlikely that this fragment corresponds to ORF1 transcription on the same DNA strand as *pdxH*. The absence of any transcription from the probe 1 *pdxH* coding strand (Fig. 2, lane 2) also demonstrated that our total RNA preparations lacked detectable DNA contamination.

Hybridization with probe 2 *pdxH-tyrS* noncoding strand showed two protected fragments of 573 ± 5 and 294 ± 5 nt (Fig. 5, lane 8). The 573-nt fragment represents full-length protection of *pdxH-tyrS* chromosomal probe 2 sequences by mRNA, where the difference in size with the undigested probe (lane 7) is due to plasmid linker sequences. Thus, there is contiguous transcription between *pdxH* and *tyrS*. Again, the coding strand control showed no transcription and no DNA contamination that could account for full-length protection of the noncoding strand probe (Fig. 5, lane 6). The molar amount of the 491-plus-480-nt P_{pdxH} transcript (lane 4) equaled that of the 573-nt *pdxH-tyrS* transcript within less than 10% experimental error (lane 8). This observation suggests that all of the *pdxH-tyrS* transcript arose from transcription initiation at P_{pdxH}.

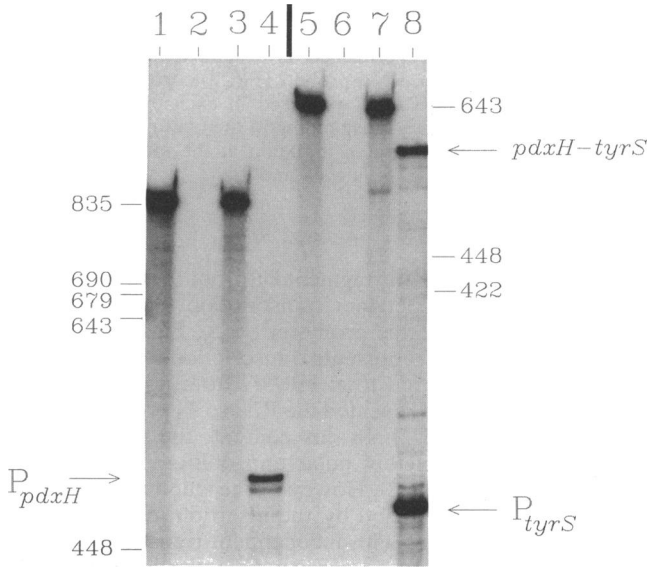

FIG. 5. RNase T_2 mapping of chromosomal transcription at the beginning of *pdxH* and from the *pdxH-tyrS* junction. Total RNA was prepared from *pdxH*$^+$ strain NU816 grown in LBC medium at 37°C with shaking as described in Materials and Methods. RNA probes 1 and 2 corresponding to the ORF1-*pdxH* and *pdxH-tyrS* junctions, respectively (Fig. 2), were synthesized from both DNA strands, and RNase T_2 protection assays of chromosomal transcripts were performed as detailed in Materials and Methods. Numbers indicate positions of RNA size standards. Lanes 1 to 4 and 5 to 8 were loaded onto the same gel at different times, which is why the standard positions are different on the two sides of the gels. Protected probe fragments corresponding to transcription initiation at the P_{pdxH} (491 ± 5 nt) and internal P_{tyrS} (295 ± 5 nt) promoters and the contiguous *pdxH-tyrS* transcript (573 ± 5 nt) are indicated. Odd-numbered or even-numbered lanes contain unhybridized RNA probes or RNA probes hybridized with total RNA, respectively. Lanes 1 and 2, probe 1 *pdxH* coding strand (i.e., probe sequence is the same as *pdxH* mRNA); lanes 3 and 4, probe 1 *pdxH* noncoding strand (i.e., probe sequence is complementary to *pdxH* mRNA); lanes 5 and 6, probe 2 *pdxH-tyrS* coding strand; lanes 7 and 8, probe 2 *pdxH-tyrS* noncoding strand.

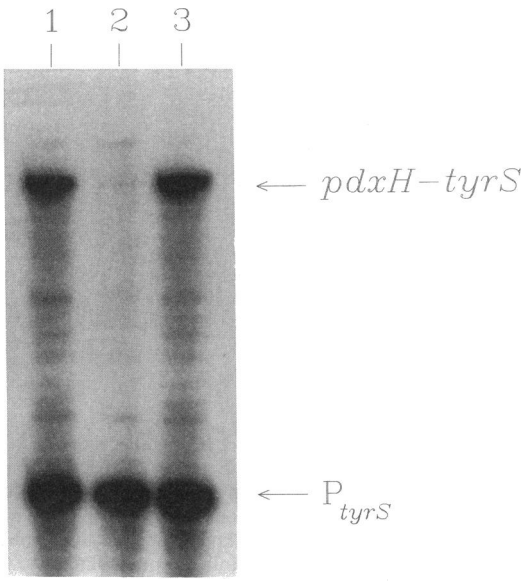

FIG. 6. Transcript analysis of *pdxH*::Mu*dI*-8 and *fis*::Km^r mutants. Total RNA was prepared from *pdxH*$^+$ parent NU816 (lane 1), *pdxH*::Mu*dI*-8 mutant NU1708 (lane 2), and *pdxH*$^+$ *fis*::Km^r mutant TX2451 (lane 3). TX2451 was grown in LBC medium, and NU816 and NU1708 were grown in LBC-PL medium with shaking at 37°C. Purification of RNA and RNase T_2 protection assays of chromosomal transcripts were performed as described for Fig. 5 and in Materials and Methods. RNA probe 2 (Fig. 2) corresponding to the *pdxH-tyrS* noncoding strand was used in each experiment. Protected probe fragments corresponding to the contiguous *pdxH-tyrS* transcript and to transcription initiation at the internal P_{tyrS} promoter are indicated (Fig. 5, lanes 7 and 8).

TABLE 2. Effect of *pdxH*::Mu*dI*-8 mutations and *pdxH*$^+$ clones on aerobic and anaerobic growth[a]

Strain(s)	Colony growth[b] on:							
	LBC medium		LBC medium-PL		MMG-CAA		MMG-CAA-PL	
	$+O_2$	$-O_2$	$+O_2$	$-O_2$	$+O_2$	$-O_2$	$+O_2$	$-O_2$
pdxH$^+$ parent (NU816)	+	+	+	+	+	+	+	+
pdxH$^+$ parent with recombinant plasmid:								
pNU216 (NU1814)	+	+	+	+	+	−	+	−
pNU217 (NU1815)	+	+	+	+	+	sm	+	sm
pTX281 (TX2268)	+	+	+	+	+	sm	+	sm
pdxH::Mu*dI*-8 mutants (NU1707, NU1708)	sm	sm	+	+	−	−	+	+
pdxH::Mu*dI*-8 mutants with recombinant plasmid:								
pNU216 (NU1730, NU1732)	+	+	+	+	+	−	+	−
pNU217 (NU1735, NU1736)	+	+	+	+	+	sm	+	sm
pTX281 (TX2277, TX2278)	+	+	+	+	+	sm	+	sm

[a] Fresh patches of each strain were made by streaking dimethyl sulfoxide-stored permanent cultures onto LBC medium (NU816), LBC medium–PL–50 μg of ampicillin per ml (*pdxH*::Mu*dI*-8 strains), or LBC medium–25 μg of chloramphenicol per ml (strains containing recombinant plasmids) plates that were incubated aerobically at 37°C overnight. Cells were then streaked from the fresh patches onto the plates indicated, which lacked antibiotic. Plates were incubated at 37°C aerobically ($+O_2$) or anaerobically ($-O_2$) in a BBL GasPak System containing an indicator strip. The same results were obtained for cells streaked onto plates containing G medium supplemented with glycerol and nitrate (52) (data not shown). Cells streaked onto control plates containing E medium supplemented with glycerol but lacking nitrate failed to grow anaerobically.

[b] +, normal-sized colonies; sm, small colonies; −, no growth. Larger colonies of strains originally containing *pdxH*$^+$ clones that arose on MMG were found to have lost the recombinant plasmids. CAA, Casamino Acids.

The 294-nt protected fragment of probe 2 (Fig. 5, lane 8) corresponds to independent transcription initiation from a relatively strong internal promoter (P_{tyrS}, Fig. 2, and 3). To prove that this band represents transcription from an internal promoter, we prepared total mRNA from a *pdxH*::Mu*dI*-8 insertion mutant and repeated the RNase T_2 protection assay (Fig. 6, lanes 1 and 2). In this context, the *pdxH*::Mu*dI*-8 insertion was completely polar and obliterated the *pdxH-tyrS* band (Fig. 6, lane 2). However, the amount of the 294-nt P_{tyrS} band was unaffected by the insertion mutation within 10% error, consistent with independent transcription initiation rather than mRNA processing. Quantitation of gel bands on a beta scope indicated that about 20% of *tyrS* steady-state transcripts originated at P_{pdxH} and 80% originated at P_{tyrS} in bacteria growing exponentially in LBC medium at 37°C. In support of this interpretation, the chemical half-lives of the *pdxH-tyrS* and P_{tyrS} transcripts were approximately the same (≈1 min) under these culture conditions following addition of 0.5 mg of rifampin per ml (data not shown). Thus, the difference in steady-state amounts of the *pdxH-tyrS* and P_{tyrS} transcripts did not appear to be caused by different transcript stabilities.

The 294-nt band is indicative of a transcription start at position 1048 in Fig. 3. Inspection of the DNA sequence in this region shows that P_{tyrS} is a nonconventional promoter, because it largely lacks −35 and −10 σ-70 consensus regions. Yet P_{tyrS} is about four times stronger than P_{pdxH}, which has relatively good consensus matches (Fig. 3). On the basis of rRNA promoters, it seemed that the unusual relative strength of P_{tyrS} might be accounted for by two upstream features. First, P_{tyrS} is preceded by A-T-rich tracks highly reminiscent of upstream activating sequences of rRNA promoters (Fig. 3) (39). The periodic repetition of A and T residues may indicate that P_{tyrS} is naturally bent DNA (21, 31, 39). Second, two putative Fis protein-binding sites are located directly upstream from P_{tyrS} (Fig. 3) (59). However, P_{tyrS} chromosomal expression was unaffected by a *fis*::*kan* mutation during growth in LBC medium at 37°C (Fig. 6, lane 3).

Requirement for PLP/PMP biosynthesis early in cell division. Growth characteristics of *pdxH*::Mu*dI*-8 mutants during mild PL limitation implied that PLP is required for a step early in cell division. *pdxH*::Mu*dI*-8 mutants show an absolute requirement for PL that cannot be satisfied by PN (Fig. 1). Although LBC rich medium seems to contain excess PN, we found that it was partially limiting for PL. Colonies of *pdxH*::Mu*dI*-8 mutants grew noticeably more slowly on LBC plates at 37°C than their *pdxH*$^+$ parent (Table 2). *pdxH*::Mu*dI*-8 mutants grown overnight in LBC medium at 30°C assumed extremely unusual shapes (Fig. 7B). The cells were greatly elongated and contained nucleoids that apparently could not segregate (compare panels A and B, Fig. 7). Several observations support the idea that the elongated cell phenotype was directly due to a limitation of PLP or PMP. Addition of PL, but not D-alanine (2, 19), to LBC medium or the presence of the pTX281 *pdxH*$^+$ minimal clone (Fig. 2) eliminated the defective cell morphology (data not shown). Moreover, the elongated cell phenotype was not caused by the presence of the Mu*dI*-8 element, because analogous *pdxA*::Mu*dI*-8 mutants did not show defective shape or

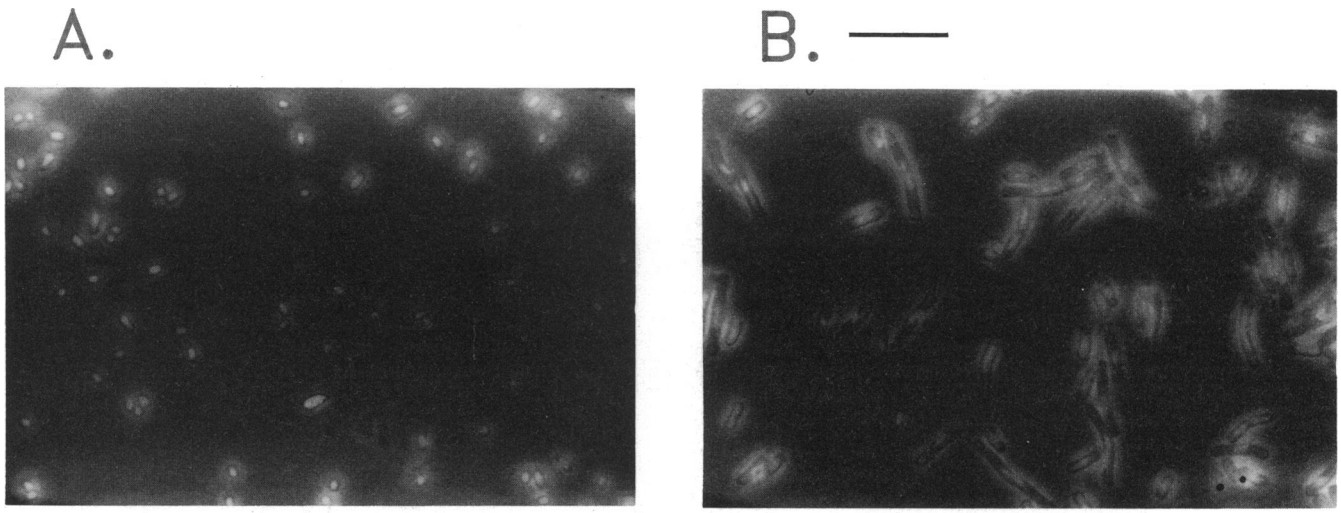

FIG. 7. Cellular morphologies of *pdxH*::Mu*dI*-8 mutant NU1707 in LBC-PL (A) or LBC (B) medium. Cells obtained from overnight cultures grown with shaking at 30°C were washed with 0.84% NaCl, stained with DAPI, and photographed under combined fluorescent and phase-contrast optics as described in Materials and Methods. Similar results were obtained for *pdxH*::Mu*dI*-8 mutant NU1708 (data not shown). Bar, 10 μm. When the *pdxH*$^+$ parent strain or *pdxH*::Mu*dI*-8 mutant NU1707 transformed with *pdxH*$^+$ plasmid pNU216, pNU217, or pTX281 was grown in LBC or LBC-PL medium, all cells resembled those in panel A (i.e., no elongated cells with partially segregated nucleoids were observed; data not shown).

nucleoid segregation (data not shown). The importance of PLP and PMP biosynthesis to cell division is considered further in the Discussion.

Requirement for *pdxH* function but existence of a second pathway for PNP oxidation. The well-characterized *pdxH*::Mu*dI*-8 insertion mutants described above allowed us to examine whether *E. coli* contains one or two forms of PdxH oxidase. In eukaryotes, PNP oxidase seems to show an absolute requirement for molecular oxygen as an electron acceptor (29, 40). Therefore, we wondered whether facultative anaerobes, such as *E. coli*, contain two forms of PNP oxidase or a single PNP oxidase with the ability to use electron acceptors other than oxygen. To test the former hypothesis, we determined whether *pdxH*::Mu*dI*-8 mutants could grow anaerobically in the absence of added PL. The results show that *pdxH*::Mu*dI*-8 mutants require PL under all growth conditions (Table 2).

The structural data presented above show that *pdxH*::Mu*dI*-8 insertions are at most only moderately polar on downstream gene expression (about 20%) because of P_{tyrS} (Fig. 6). In addition, transcription downstream of *tyrS* probably occurs from the opposite DNA strand from *pdxH* and *tyrS*, which means that *tyrS* is the last gene in what appears to be a two-gene complex operon (Fig. 2 and see above). Thus, it seemed extremely unlikely that *pdxH*::Mu*dI*-8 insertions were exerting a polar effect on a downstream, anaerobic *pdxH* gene. To test this notion further, we transformed the *pdxH*$^+$ parent NU816 and *pdxH*::Mu*dI*-8 mutants NU1707 and NU1708 with the three *pdxH*$^+$ plasmids depicted in Fig. 2. Surprisingly, pNU217 and minimal *pdxH*$^+$ clone pTX281 inhibited and pNU216 prevented anaerobic growth of both the parent and *pdxH* mutants in Casamino Acid-supplemented MMG lacking antibiotics (Table 2). When larger colonies did appear, the bacteria had lost the *pdxH*$^+$ plasmids. By contrast, on LBC rich medium, the plasmids did not adversely affect growth. Control experiments indicated that the pBR325 vector did not adversely affect anaerobic growth of the NU816 parent strain (data not shown). Thus, *pdxH*$^+$ itself and other genes nearby cannot be tolerated on multicopy plasmids in bacteria growing anaerobically on enriched minimal-glucose medium.

Last, we tested whether suppressors could be isolated in *pdxH*::Mu*dI*-8 mutants that allow aerobic or anaerobic growth on minimal media lacking PL. Unexpectedly, stable, spontaneous suppressors could be isolated both in the presence and absence of oxygen. *pdxH* suppressors isolated under aerobic conditions allowed anaerobic growth without PL and vice versa (data not shown). Preliminary cotransduction mapping revealed at least two classes of suppressors, linked or unlinked to the *pdxH* region, which were isolated most readily under anaerobic or aerobic conditions, respectively (data not shown). Implications to PLP biosynthesis of suppressors that replace *pdxH* oxidase function are considered in the Discussion.

***pdxH*::Mu*dI*-8 mutants excrete significant amounts of L-Glu and a compound that triggers L-valine inhibition of *E. coli* K-12 strains.** Mutations in *pdxH* lead to accumulation of precursors in the PLP biosynthetic pathway, such as PNP and PMP (Fig. 1). We observed that *pdxH*::Mu*dI*-8 liquid cultures grew about a third as fast as the *pdxH*$^+$ parent strain in MMG-PL at 30°C (data not shown). When *pdxH*::Mu*dI*-8 mutants were streaked side by side with their *E. coli* K-12 parent strain on MMG-PL plates, a striking inhibition of the parent strain was obvious (data not shown). These results strongly hinted that *pdxH*::Mu*dI*-8 mutants were excreting a growth inhibitor into the culture medium.

To investigate this phenomenon further, cell-free filtrates were made from cultures of *pdxH*::Mu*dI*-8 mutants (Table 3). Ten microliters of filtrate from overnight cultures was sufficient to cause a 1- to 2-cm-diameter inhibition zone for K-12 strain NU816. Because inhibition was observed only on MMG agar but not on LBC rich agar, it seemed that the inhibitor might be acting on some biosynthetic process. Moreover, production of inhibitor was due solely to the *pdxH* mutations, since no inhibition was observed for

TABLE 3. Growth inhibition by medium filtrates of *pdxH*::Mu*dI*-8 mutants

Filtrate source[a]	Diam of inhibition zone (cm) of[b]:					
	E. coli K-12		*E. coli* B		Filtrate-resistant K-12 mutant	
	−Ile	+Ile	−Ile	+Ile	−Ile	+Ile
pdxH$^+$ parent (NU816)	0	NT	0	NT	NT	NT
pdxH::Mu*dI*-8 mutants						
NU1707	1.4	0	0	0	0	0
NU1708	2.2	0	0	0	0	0
pdxA::Mu*dI*-8 (NU1709)	0	NT	NT	NT	NT	NT
pdxH::Mu*dI*-8 mutants with recombinant *pdxH*$^+$ plasmids	0	NT	NT	NT	NT	NT
Chemicals (mg/ml)						
L-Val						
0.3	1.8	0	0	0	0	0
0.03	1.1	0	0	0	0	0
0.003	0	0	0	0	0	0
L-Glu (3)	0	NT	NT	NT	NT	NT
L-Val + L-Glu						
0.03 + 3	1.1	NT	NT	NT	NT	NT
0.003 + 3	0	NT	NT	NT	NT	NT
α-KIV						
0.3	2.1	0	NT	NT	NT	NT
0.03	1.2	0	NT	NT	NT	NT

[a] Cultures used to prepare filtrates were grown in MMG-PL at 30°C for 3 days (*pdxH*::Mu*dI*-8 mutants) or 1 to 2 days (other strains). Ampicillin (12.5 μg/ml) was added to all cultures except NU816. Cells were then removed by low-speed centrifugation followed by filtration through 0.2-μm-pore-size filters.

[b] Cultures of the three strains to be tested were grown in MMG overnight at 37°C. The overnight culture (0.1 ml) was mixed with 0.8% MMG soft agar and poured onto 1.5% MMG bottom agar. Both top and bottom agars contained 0.3 mM L-Ile, where indicated. Inhibition caused by cell filtrates and various chemicals was tested by adding 10 μl of filtrates or chemical solutions at the concentrations listed to sterile filter paper discs placed on plate surfaces immediately after the agar hardened. Plates were inverted and incubated at 37°C for 1 day before inhibition zones were measured. NT, not tested.

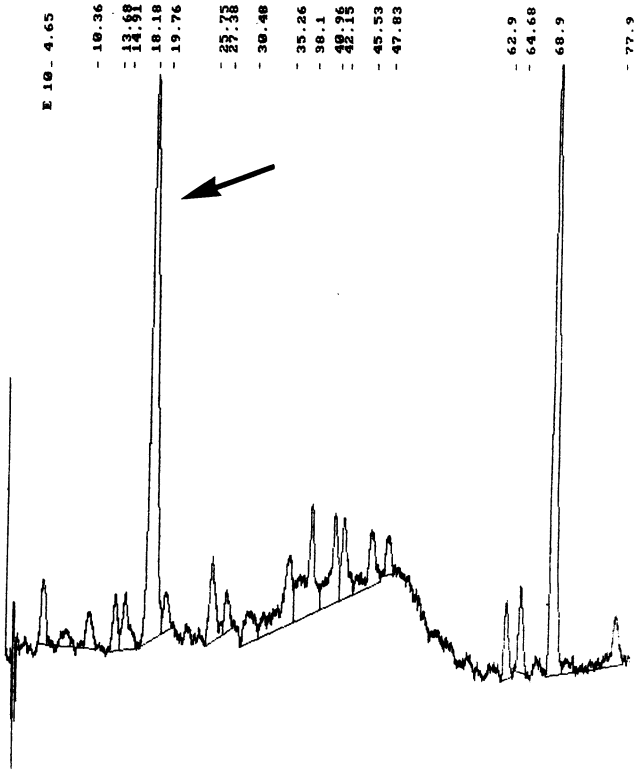

FIG. 8. HPLC analysis of amino acids contained in cell filtrates of a *pdxH*::Mu*dI*-8 mutant (NU1708) grown in MMG-PL at 37°C with shaking. Cell filtrates were prepared as described in Table 2, footnote *a*. The sterile conditioned medium was further filtered through a Centricon 3 filter (Amicon Corp., Beverly, Mass.) to remove molecules with molecular masses greater than 3,500 Da. This extra filtration did not appear to diminish the filtrate's ability to inhibit *E. coli* K-12 (data not shown). The final filtrate was mixed with low concentrations of amino acid standards to help identify peaks and subjected to HPLC ion-exchange chromatography as described in Materials and Methods. The large peak at 18.18 min (arrow) represents L-Glu. The other large peak at 68.9 min is ammonium ion. The L-Val standard is at 35.26 min. Only the two large peaks were observed on chromatograms of conditioned medium lacking the amino acid standards (data not shown). Additional details and controls are described in the text.

pdxA::Mu*dI*-8 or *pdxH*::Mu*dI*-8 (*pdxH*$^+$ plasmid) strains (Table 3).

L-Valine is a well-known metabolic inhibitor of *E. coli* K-12 growth that acts by feedback inhibiting isozymes I and III of acetohydroxy acid synthase (57). The following properties of the culture filtrates strongly suggested that the excreted inhibitor was L-Val or a compound related to L-Val (Table 3): (i) L-Ile reversed the inhibitory effect, (ii) *E. coli* K-12, but not *E. coli* B, cells were inhibited, and (iii) 2-aminopurine mutagenized *E. coli* K-12 mutants selected for resistance to the *pdxH* mutant filtrates were also resistant to L-Val inhibition.

We tested whether *pdxH* mutants were excreting L-Val by performing amino acid analyses on filtrates (Fig. 8). The MMG-PL culture filtrate of *pdxH* mutant NU1707 or NU1708 was mixed with a low concentration of amino acid standards to pinpoint relative peak positions. The resulting chromatograms showed two major peaks corresponding to ammonium ion and L-glutamate (arrow, Fig. 8) but no peak of L-Val (Fig. 8). When amino acid standards were omitted, only the ammonium and L-glutamate peaks were seen (data not shown). Inhibition zone tests with pure L-Val suggested that if L-Val were present, it would have a minimal concentration of approximately 0.03 mg/ml (Table 3). This concentration was well within the range of detection of the amino acid analyses (data not shown).

Excretion of L-Glu by *pdxH*::Mu*dI*-8 mutants was totally unanticipated (Fig. 8). L-Glu was not detected in filtrates of the *pdxH*$^+$ parent (NU816) or *pdxH*::Mu*dI*-8 mutants containing a *pdxH*$^+$ recombinant plasmid (NU2352 and NU2353) (data not shown). The presence of L-Glu in culture filtrates was confirmed further with a bioassay employing the enzyme glutamate dehydrogenase, which specifically uses L-Glu as its substrate (6). Our results showed that NU1708 (*pdxH*), but not NU816 (*pdxH*$^+$), filtrates indeed contained a substrate of glutamate dehydrogenase (data not shown). Based on the amino acid analyses, the concentration of L-Glu in NU1708 filtrates was about 1 nmol/μl (≈0.15 mg/ml). The effects of pure L-Glu on the growth of *E. coli* K-12 strains were also tested. No inhibition zone was seen even with L-Glu concentrations as high as 3 mg/ml. In addition, L-Glu did not enhance the inhibitory effect of L-Val (Table 3). On the basis of these results, L-Glu was not the inhibitor of *E. coli* K-12 growth excreted by *pdxH* mutants.

Since L-Val was not excreted and L-Glu did not act as an inhibitor, it seemed likely that a precursor of L-Val lacking a free amino group might be the inhibitor released by *pdxH* mutants. Such a precursor could then be taken up by *E. coli* K-12 strains and converted directly into L-Val, thereby eliciting inhibition. To account for the simultaneous excretion of L-Glu and this precursor, we hypothesized that PNP/PMP accumulation in *pdxH* mutants (Fig. 1) inhibits the activity of transaminases, which use L-Glu as a common substrate. In the L-Val biosynthetic pathway, blockage of the transaminase reaction would lead to accumulation and possibly excretion of the keto acid α-ketoisovalerate (α-KIV). Consistent with this hypothesis, we found that α-KIV inhibited the growth of *E. coli* K-12 cells in a manner similar to L-Val (Table 3).

DISCUSSION

PNP oxidase, which catalyzes the last step in PLP biosynthesis in all organisms (Fig. 1), has been extensively characterized biochemically in animal tissues (10, 11, 29, 36). In this paper, we report a molecular genetic analysis of *pdxH*, which encodes PNP oxidase in *E. coli* K-12. These studies revealed significant new information about the function, genetic organization, and physiological role of *E. coli* PdxH oxidase.

We found several similarities between *E. coli* and eukaryotic PNP oxidases. The predicted monomer molecular mass of the *E. coli* polypeptide was 25,545 Da (Fig. 3), which is similar to that of the eukaryotic enzyme. Likewise, the predicted amino acid composition of *E. coli* PdxH oxidase (Fig. 3) was similar to that of eukaryotic enzymes, which were determined biochemically (36). The *E. coli* PdxH polypeptide is predicted to be basic (pI≈9.6) and to contain a relatively high number of polar amino acids compared to aromatic and sulfur-containing residues. *E. coli* PNP oxidase probably binds FMN, as indicated by its full-length homology with the FMN-binding FprA protein of *M. xanthus* (Fig. 4) (20). It is well established that eukaryotic PNP oxidases use FMN as a cofactor (11). Furthermore, the high degree (>40% identity) and nearly full-length homology between PdxH and FprA is striking (Fig. 4) and strongly implies that FprA is PNP oxidase of *M. xanthus*.

One fundamental difference between the *E. coli* and eukaryotic oxidases may concern function during anaerobic growth. Eukaryotic PdxH oxidases are thought to utilize molecular oxygen as their sole electron acceptor (29, 40). Our genetic analyses show that PdxH oxidase is required in wild-type *E. coli* K-12 for both aerobic and anaerobic growth (Table 2). Consistent with this interpretation, crude extracts from the NU1708 *pdxH*::Mu*dI*-8 insertion mutant totally lack the PNP oxidase activity, which is easily detectable from its $pdxH^+$ parent (66). However, the existence of suppressors of *pdxH* function in *pdxH* insertion mutants (see Results) suggests a more complicated situation. One possibility is that there is a single form of PdxH oxidase in wild-type *E. coli*, which uses oxygen aerobically and another electron acceptor anaerobically. In this case, *pdxH* suppressors arise by mutational change in specificity of a pathway that does not normally participate in PNP oxidation. Alternatively, a cryptic pathway for PNP oxidation might be activated. A second possibility is that PdxH protein is the aerobic oxidase that is nevertheless required for activation of a second, anaerobic form of the enzyme. According to this model, *pdxH* suppressors arise because of constitutive expression of the second form of oxidase. Enzymological characterization of *E. coli* PdxH and molecular genetic analysis of *pdxH* suppressors are in progress to test these models.

Genetic, structural, and in vivo transcript analyses revealed that *pdxH* forms a complex operon with downstream *tyrS* (Fig. 2, 3, 5, and 6). In LBC medium at 37°C with aeration, approximately 20 or 80% of steady-state *tyrS* transcripts seemed to originate from the *pdxH* (P_{pdxH}) or *tyrS* (P_{tyrS}) promoters, respectively (Fig. 2, 3, 5, and 6). No transcription was detected in either direction in the 280-bp region immediately upstream from the start of *pdxH* transcription, although this region contained an open reading frame (ORF1, Fig. 2 and 3). Gene fusions immediately downstream from *tyrS* indicated that this region is transcribed in the opposite direction to *tyrS* (Fig. 2). Thus, *pdxH* and *tyrS* form a two-gene complex operon that contains a relatively strong internal promoter (P_{tyrS}). This conclusion means that all known genes involved in PN (vitamin B_6) or PLP biosynthesis are members of a complex, multifunctional operon (2, 17, 33, 34, 44, 54). Besides *tyrS*, other aminoacyl-tRNA synthetase genes have also been found in complex operons (27, 28, 35). One model to explain this arrangement is that complex operons may allow coordinated or differential expression of key metabolic functions depending on the physiological state of the cell. In this regard, it is interesting that *pdxA*, *pdxB*, and now *pdxH* are in complex operons with genes that encode proteins important for translation, and *pdxJ* is in a complex operon with a recently discovered essential gene of unknown function (33, 54).

The regulation of *tyrS* has not been extensively studied in *E. coli*. On the basis of precedents from other aminoacyl-tRNA synthetase genes, *tyrS* may be regulated positively by growth rate and perhaps by tyrosine limitation (38). *Bacillus subtilis tyrS* is induced by tyrosine starvation possibly through a mechanism involving antitermination (61). The results presented here suggest that *E. coli tyrS* is transcribed mainly from a relatively powerful, nonconventional internal promoter that shares features with rRNA promoters (39) (Fig. 3). Although P_{tyrS} lacks strong −35 and −10 consensus sequences, it is preceded by A-T-rich DNA that likely is naturally bent (21, 31, 39) and contains two potential Fis protein-binding sites (59). However, in vivo transcription from P_{tyrS} was unaffected by a *fis*::*kan* mutation (Fig. 6), which is a property shown by several other promoters that bind Fis in vitro (65). P_{pdxH} accounts for *pdxH* and about 20% of *tyrS* transcription (Fig. 5 and 6) and appears to be a conventional σ-70 promoter. PDX boxes, found near the starts of *pdxA*, *pdxB*, and *pdxJ* (33, 44, 49), and other putative regulatory motifs were not discernable around P_{pdxH} or within *pdxH*. Ongoing experiments should determine whether relative steady-state amounts or rates of transcription from P_{pdxH} and P_{tyrS} change under different growth conditions.

pdxH::Mu*dI*-8 insertion mutants showed several unusual phenotypic properties that seemed to be due directly to PLP coenzyme level rather than partial polarity on *tyrS* expression. When *pdxH* mutants ran out of PL in LBC rich medium, they showed a pronounced division defect characterized by elongated large cells with unsegregated nucleoids (Fig. 7). This appearance contrasts with the spherical cell and swelling and bleb phenotypes caused by severe PLP limitation that presumably reflects blockage of peptidoglycan biosynthesis (2, 19). The cell division defect reported here was not lessened by D-alanine addition and may not reflect a block in murein biosynthesis (2, 19). The unsegregated nucleoids in mildly PLP-limited *pdxH* mutants suggest

that some early step in cell division requires PLP (12, 16). This conclusion implies that *E. coli* needs to carefully regulate PLP level throughout the cell cycle. Consistent with this interpretation, *pdxA* and *pdxB*, which are required for PN and PLP biosynthesis (2, 44), are positively regulated by growth rate at the level of transcription initiation (43). In this regard, it is interesting that *fprA*, which we show probably encodes PNP oxidase (Fig. 4), has been reported to be developmentally regulated in *M. xanthus* (20). If this interpretation is correct, PLP coenzyme level may be modulated as a function of developmental stage in *M. xanthus*.

Excretion of appreciable amounts of L-glutamate and a precursor of L-valine by *pdxH* mutants in media containing PL (Fig. 8; Table 3) underscores the importance to cells of maintaining appropriate pool levels of PLP precursors. *pdxH* mutants most likely accumulate PNP and PMP, which are substrates of PNP oxidase (Fig. 1). PNP and PMP are known to be potent inhibitors of PLP-dependent enzymes, including transaminases (52), and transaminases utilize L-Glu as a common substrate (5). We speculate that PNP and PMP accumulation by *pdxH* mutants inhibits transaminases and leads to the accumulation and excretion of transaminase substrates, including L-Glu and α-keto acids, such as the immediate precursor of L-Val, α-KIV. This hypothesis has two implications. First, under some circumstances, cellular PNP or PMP concentrations control the activity of certain enzymes and thereby regulate the flow of intermediates in certain metabolic pathways. Second, excretion of L-Glu implies an unanticipated breakdown in feedback regulation of L-Glu biosynthesis (42). In this case, the PNP level may affect metabolic flow by altering the efficiency of feedback control. Whether PNP and PLP levels are modulated in *pdxH*$^+$ bacteria under different growth conditions awaits testing.

ACKNOWLEDGMENTS

We thank the colleagues listed in Table 1 for bacterial strains and plasmid clones. Tsz-Kwong Man provided valuable assistance in the analysis of *pdxH* suppressors. We also thank D. M. Connolly, W. B. Dempsey, H.-C. E. Leung, A. J. Pease, B. B. Roa, H.-C. T. Tsui, and G. Zhao for discussions and comments.

This work was supported by Public Health Service grant GM37561 from the National Institute of General Medical Sciences.

REFERENCES

1. **Arps, P. J., and M. E. Winkler.** 1987. Structural analysis of the *Escherichia coli* K-12 *hisT* operon by using a kanamycin resistance cassette. J. Bacteriol. **169:**1061–1070.
2. **Arps, P. J., and M. E. Winkler.** 1987. An unusual genetic link between vitamin B_6 biosynthesis and tRNA pseudouridine modification in *Escherichia coli* K-12. J. Bacteriol. **169:**1071–1079.
3. **Ausubel, F. M., R. Brent, R. E. Kingston, D. D. Moore, J. G. Seidman, J. A. Smith, and K. Struhl.** 1989. Current protocols in molecular biology. Wiley Interscience, New York.
4. **Barker, D. G., C. J. Bruton, and G. Winter.** 1982. The tyrosyl-tRNA synthetase from *Escherichia coli*. Complete nucleotide sequence of the structural gene. FEBS Lett. **150:**419–423.
5. **Bender, D. A.** 1985. Amino acid metabolism. John Wiley & Sons, Inc., New York.
6. **Bernt, E., and H.-U. Bergmeyer.** 1965. L-Glutamate: determination with glutamic dehydrogenase, p. 384–388. *In* H.-U. Bergmeyer (ed.), Methods of enzymatic analysis. Academic Press, Inc., New York.
7. **Birktoft, J. J., and L. J. Banaszak.** 1984. Structure-function relationships among nicotinamide-adenine dinucleotide oxidoreductases. Peptide Protein Rev. **4:**1–46.
8. **Bolivar, F.** 1978. Construction and characterization of new cloning vehicles. III. Derivatives of plasmid pBR322 carrying unique *Eco*RI generated recombinant molecules. Gene **2:**95–113.
9. **Castilho, B. A., P. Olfson, and M. J. Casadaban.** 1984. Plasmid insertion mutagenesis and *lac* gene fusion with mini-Mu bacteriophage transposons. J. Bacteriol. **158:**488–495.
10. **Choi, S.-Y., J. E. Churchich, E. Zaiden, and F. Kwok.** 1987. Brain pyridoxine-5-phosphate oxidase: modulation of its catalytic activity by reaction with pyridoxal 5-phosphate and analogs. J. Biol. Chem. **262:**12013–12017.
11. **Churchich, J. E.** 1984. Brain pyridoxine-5-phosphate oxidase. A dimeric enzyme containing one FMN site. Eur. J. Biochem. **138:**327–332.
12. **Cooper, S.** 1991. Bacterial growth and division: biochemistry and regulation of prokaryotic and eukaryotic division cycles. Academic Press, Inc., New York.
13. **Davis, R. W., D. Botstein, and J. R. Roth.** 1980. Advanced bacterial genetics. Cold Spring Harbor Laboratory, Cold Spring Harbor, N.Y.
14. **Dempsey, W. B.** 1966. Synthesis of pyridoxine by a pyridoxal auxotroph of *Escherichia coli*. J. Bacteriol. **92:**333–337.
15. **Dempsey, W. B.** 1987. Synthesis of pyridoxal phosphate, p. 539–543. *In* F. C. Neidhardt, J. L. Ingraham, K. B. Low, B. Magasanik, M. Schaechter, and H. E. Umbarger (ed.), *Escherichia coli* and *Salmonella typhimurium*: cellular and molecular biology. American Society for Microbiology, Washington, D.C.
16. **Donachie, W. D., K. J. Begg, and N. F. Sullivan.** 1984. Morphogenes of *Escherichia coli*, p. 27–62. *In* R. Losick and L. Shapiro (ed.), Microbial development. Cold Spring Harbor Laboratory, Cold Spring Harbor, N.Y.
17. **Duncan, K., and J. R. Coggins.** 1986. The *serC-aroA* operon of *Escherichia coli*: a mixed function operon encoding enzymes from two different amino acid biosynthetic pathways. Biochem. J. **234:**49–57.
18. **Erickson, J. W., V. Vaughn, W. A. Walter, F. C. Neidhardt, and C. A. Gross.** 1987. Regulation of the promoters and transcripts of *rpoH*, the *Escherichia coli* heat shock regulatory gene. Genes Dev. **1:**419–432.
19. **Grogan, D. W.** 1988. Temperature-sensitive murein synthesis in an *Escherichia coli pdx* mutant and the role of alanine racemase. Arch. Microbiol. **150:**363–367.
20. **Hagen, T. J., and L. J. Shimkets.** 1990. Nucleotide sequence and transcriptional products of the *csg* locus of *Myxococcus xanthus*. J. Bacteriol. **172:**15–23.
21. **Hagerman, P. J.** 1986. Sequence-directed curvature of DNA. Nature (London) **321:**449–450.
22. **Hedrick, J. L., and E. H. Fischer.** 1965. On the role of pyridoxal 5′-phosphate in phosphorylase. I. Absence of classical vitamin B_6-dependent enzymatic activities in muscle glycogen phosphorylase. Biochemistry **4:**1337–1342.
23. **Hill, R. E., B. G. Sayer, and I. D. Spenser.** 1989. Biosynthesis of vitamin B_6: incorporation of D-1-deoxyxylulose. J. Am. Chem. Soc. **111:**1916–1917.
24. **Hiraga, S., H. Niki, T. Ogara, C. Ichinose, H. Mori, B. Ezaki, and A. Jaffe.** 1989. Chromosome partitioning in *Escherichia coli*: novel mutants producing anucleate cells. J. Bacteriol. **171:**1496–1505.
25. **Hockney, R. C., and T. Scott.** 1979. The isolation and characterization of three types of vitamin B6 auxotrophs of *Escherichia coli* K12. J. Gen. Microbiol. **110:**275–283.
26. **Hughes, K. T., and J. R. Roth.** 1989. Conditionally transposition-defective derivative of Mu *d*1(Amp Lac). J. Bacteriol. **159:**130–137.
27. **Kamio, Y., C.-K. Lin, M. Regue, and H. C. Wu.** 1985. Characterization of the *ileS-lsp* operon in *Escherichia coli*: identification of an open reading frame upstream of the *ileS* gene and potential promoter(s) for the *ileS-lsp* operon. J. Biol. Chem. **260:**5616–5620.
28. **Kawakami, K., Y. H. Jonsson, G. R. Bjork, H. Ikeda, and Y. Nakamura.** 1988. Chromosomal location and structure of the operon encoding peptide-chain-release factor 2 of *Escherichia coli*. Proc. Natl. Acad. Sci. USA **85:**5620–5624.
29. **Kazarinoff, M. N., and D. B. McCormick.** 1975. Rabbit liver pyridoxamine (pyridoxine) 5′-phosphate oxidase. Purification and properties. J. Biol. Chem. **250:**3436–3442.

30. **Kim, Y. T., and J. E. Churchich.** 1989. Activation of a flavoprotein by proteolysis. J. Biol. Chem. **264:**15751–15753.
31. **Koo, H.-S., H.-M. Wu, and D. M. Crothers.** 1986. DNA bending at adenine-thymine tract. Nature (London) **320:**501–506.
32. **Kwok, F., and J. E. Churchich.** 1980. Interaction between pyridoxal kinase and pyridoxine-5-P oxidase, two enzymes involved in the metabolism of vitamin B_6. J. Biol. Chem. **255:**882–887.
33. **Lam, H.-M., E. Tancula, W. B. Dempsey, and M. E. Winkler.** 1992. Suppression of insertions in the complex *pdxJ* operon of *Escherichia coli* K-12 by *lon* and other mutations. J. Bacteriol. **174:**1554–1567.
34. **Lam, H.-M., and M. E. Winkler.** 1990. Metabolic relationships between pyridoxine (vitamin B_6) and serine biosynthesis in *Escherichia coli* K-12. J. Bacteriol. **172:**6518–6528.
35. **Mayaux, J.-F., G. Fayat, M. Fromant, M. Springer, M. Grunberg-Manago, and S. Blanquet.** 1983. Structural and transcriptional evidence for related *thrS* and *infC* expression. Proc. Natl. Acad. Sci. USA **80:**6152–6156.
36. **McCormick, D. B., and A. H. Merrill.** 1980. Pyridoxamine (pyridoxine) 5'-phosphate oxidase, p. 1–26. *In* G. P. Tryfiates (ed.), Vitamin B6 metabolism and role in growth. Food Nutrition Press, Westport, Conn.
37. **Miller, J. H.** 1972. Experiments in molecular genetics. Cold Spring Harbor Laboratory, Cold Spring Harbor, N.Y.
38. **Neidhardt, F. C., J. Parker, and W. G. McKeever.** 1975. Function and regulation of aminoacyl-tRNA synthetases in prokaryotic and eukaryotic cells. Annu. Rev. Microbiol. **29:** 215–250.
39. **Plaskon, R. R., and R. M. Wartell.** 1987. Sequence distributions associated with DNA curvature are found upstream of strong *E. coli* promoters. Nucleic Acids Res. **15:**785–796.
40. **Pogell, B. M.** 1958. Enzymatic oxidation of pyridoxamine phosphate to pyridoxal phosphate in rabbit liver. J. Biol. Chem. **232:**761–776.
41. **Porter, T. D., and C. B. Kasper.** 1986. NADPH-cytochrome P-450 oxidoreductase: flavin mononucleotide and flavin adenine dinucleotide domains evolved from different flavoproteins. Biochemistry **25:**1682–1687.
42. **Reitzer, L. J., and B. Magasanik.** 1987. Ammonia assimilation and the biosynthesis of glutamine, glutamate, aspartate, asparagine, L-alanine, and D-alanine, p. 302–320. *In* F. C. Neidhardt, J. L. Ingraham, K. B. Low, B. Magasanik, M. Schaechter, and H. E. Umbarger (ed.), *Escherichia coli* and *Salmonella typhimurium*: cellular and molecular biology. American Society for Microbiology, Washington, D.C.
43. **Roa, B. B., K. Betchel, and M. E. Winkler.** 1992. Unpublished observation.
44. **Roa, B. B., D. M. Connolly, and M. E. Winkler.** 1989. Overlap between *pdxA* and *ksgA* in the complex *pdxA-ksgA-apaG-apaH* operon of *Escherichia coli* K-12. J. Bacteriol. **171:**4767–4777.
45. **Rudd, K. E.** Alignment of *E. coli* DNA sequences to a revised, integrated genomic restriction map. *In* J. Miller (ed.), A short course in bacterial genetics: a laboratory manual and handbook of *Escherichia coli* and related bacteria, in press. Cold Spring Harbor Laboratory Press, Cold Spring Harbor, N.Y.
46. **Sambrook, J., E. F. Fritsch, and T. Maniatis.** 1989. Molecular cloning: a laboratory manual, 2nd ed. Cold Spring Harbor Laboratory, Cold Spring Harbor, N.Y.
47. **Sanger, F., S. Nicklen, and A. R. Coulson.** 1977. DNA sequencing with chain-terminating inhibitors. Proc. Natl. Acad. Sci. USA **74:**5463–5467.
48. **Schlesinger, S., and E. W. Nester.** 1969. Mutants of *Escherichia coli* with an altered tyrosyl-transfer ribonucleic acid synthetase. J. Bacteriol. **100:**167–175.
49. **Schoenlein, P. V., B. B. Roa, and M. E. Winkler.** 1989. Divergent transcription of *pdxB* and homology between the *pdxB* and *serA* gene products in *Escherichia coli* K-12. J. Bacteriol. **171:**6084–6092.
50. **Shimkets, L. J.** 1990. The *Myxococcus xanthus* FprA protein causes increased flavin biosynthesis in *Escherichia coli*. J. Bacteriol. **172:**24–30.
51. **Snell, E. E.** 1955. Chemical structure in relation to biological activities of vitamin B_6. Vitam. Horm. **16:**77–113.
52. **Spencer, M. E., and J. R. Guest.** 1974. Proteins of the inner membrane of *Escherichia coli*: changes in composition associated with anaerobic growth and fumerate reductase amber mutations. J. Bacteriol. **117:**954–959.
53. **Stockman, B. J., A. M. Krezel, and J. L. Markley.** 1990. Hydrogen-1, carbon-13, and nitrogen-15 NMR spectroscopy of *Anabaena* 7120 flavodoxin: assignment of beta-sheet and flavin binding site resonances and analysis of protein-flavin interactions. Biochemistry **29:**9600–9609.
54. **Takiff, H. E., T. Baker, T. Copeland, S.-M. Chen, and D. L. Court.** 1992. Locating essential *Escherichia coli* genes by using mini-Tn*10* transposons: the *pdxJ* operon. J. Bacteriol. **174:**1544–1553.
55. **Tryfiates, G. P.** 1986. Pyridoxal phosphate and metabolism, p. 421–448. *In* D. Dolphin, R. Poulson, and O. Avramovic (ed.), Vitamin B_6 pyridoxal phosphate, part B. Wiley Interscience, New York.
56. **Turner, J. M., and F. C. Happold.** 1961. Pyridoxamine phosphate-oxidase and pyridoxal phosphate-phosphatase activities in *Escherichia coli*. Biochem. J. **78:**364–372.
57. **Umbarger, H. E.** 1987. Biosynthesis of the branched-chain amino acids, p. 352–367. *In* F. C. Neidhardt, J. L. Ingraham, K. B. Low, B. Magasanik, M. Schaechter, and H. E. Umbarger (ed.), *Escherichia coli* and *Salmonella typhimurium*: cellular and molecular biology. American Society for Microbiology, Washington, D.C.
58. **Uyeda, K.** 1969. Reaction of phosphofructokinase with maleic anhydride, succinic anhydride, and pyridoxal 5'-phosphate. Biochemistry **8:**2366–2373.
59. **Verbeek, H., L. Nilsson, G. Baliko, and L. Bosch.** 1990. Potential binding sites of the trans-activator FIS are present upstream of all rRNA operons and of many but not all tRNA operons. Biochim. Biophys. Acta **1050:**302–306.
60. **Wada, H., and E. E. Snell.** 1961. The enzymatic oxidation of pyridoxine and pyridoxamine phosphates. J. Biol. Chem. **236:** 2089–2095.
61. **Waye, M. M. Y., and G. Winter.** 1986. A transcription terminator in the 5' non-coding region of the tyrosyl tRNA synthetase gene from *Bacillus stearothermophilus*. Eur. J. Biochem. **158:** 505–510.
62. **White, R. S., and W. B. Dempsey.** 1970. Purification and properties of vitamin B_6 kinase from *Escherichia coli* B. Biochemistry **9:**4057–4064.
63. **Winans, S. C., S. J. Elledge, J. H. Krueger, and G. C. Walker.** 1985. Site-directed insertion and deletion mutagenesis with cloned fragments in *Escherichia coli*. J. Bacteriol. **161:**1219–1221.
64. **Yasunobu, K. T., and M. Tanaka.** 1980. The isolation and primary structures of various types of ferredoxin. Methods Enzymol. **69:**228–238.
65. **Zacharias, M., H. U. Goringer, and R. Wagner.** 1992. Analysis of the Fis-dependent and Fis-independent transcription activation mechanisms of the *Escherichia coli* ribosomal RNA P1 promoter. Biochemistry **31:**2621–2628.
66. **Zhao, G., and M. E. Winkler.** 1992. Unpublished observation.